Journal of Medicinal Chemistry

ARTICLE

pubs.acs.org/jmc

Identification and Biological Activities of New Taccalonolide Microtubule Stabilizers

Jiangnan Peng,*[,†] April L. Risinger,[†] Gary A. Fest,[†] Evelyn M. Jackson,[†] Gregory Helms,[‡] Lisa A. Polin,[§] and Susan L. Mooberry*[,†]

[†]Department of Pharmacology, University of Texas Health Science Center at San Antonio, San Antonio, Texas 78229, United States

[‡]Nuclear Magnetic Resonance Center, Department of Chemistry, Washington State University, Pullman, Washington 99164, United States

[§]Department of Oncology, Barbara Ann Karmanos Cancer Institute, Wayne State University School of Medicine, Detroit, Michigan 48201, United States

Supporting Information

ABSTRACT: The taccalonolides are a unique class of microtubule stabilizers that do not bind directly to tubulin. Three new taccalonolides, Z, AA, and AB, along with two known compounds, taccalonolides R and T, were isolated from *Tacca chantrieri* and *Tacca integrifolia*. Taccalonolide structures were determined by 1D and 2D NMR methods. The biological activities of the new taccalonolides, as well as taccalonolides A, B, E, N, R, and T, were evaluated. All nine taccalonolides display microtubule stabilizing activity, but profound differences in antiproliferative potencies were noted, with IC_{50} values ranging from the low nanomolar range for taccalonolide AA (32 nM) to the low micromolar range for taccalonolide R (13 μM). These studies demonstrate that diverse taccalonolides possess microtubule stabilizing properties and that significant structure−activity relationships exist. In vivo antitumor evaluations of taccalonolides A, E, and N show that each of these molecules has in vivo antitumor activity.

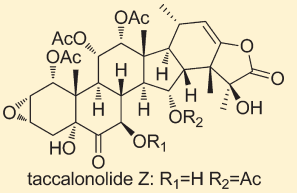

taccalonolide Z: R_1=H R_2=Ac
taccalonolide AA: R_1=R_2=Ac
taccalonolide AB: R_1=R_2=H

INTRODUCTION

Microtubule stabilizers are one of the most important classes of anticancer therapeutics used in the clinic today. The taxoid microtubule stabilizer paclitaxel has been widely used in the treatment of solid tumors, including breast, ovarian, and lung cancers for over a decade as a single agent and in combination with targeted therapies. In spite of their clinical utility, the shortcomings of paclitaxel and the second generation semisynthetic taxoid, docetaxel, include innate and acquired drug resistance and dose limiting toxicities.[1] Two new microtubule stabilizers have been approved for clinical use in the past 3 years: the epothilone ixabepilone and the taxoid cabazitaxel, which circumvent some but not all of the shortcomings of first and second generation microtubule stabilizers.[2,3] These microtubule stabilizing drugs all bind to the interior lumen of the intact microtubule at the taxoid binding site, which causes a stabilization of microtubule protofilament interactions and thereby decreases the dynamic nature of microtubules.[4]

Two additional classes of microtubule stabilizers that do not bind within the taxoid site have been isolated from nature: laulimalides/peloruside A and the taccalonolides. Laulimalide and peloruside A have recently been shown to bind to the exterior of the microtubule at a site distinct from the taxoid binding site but result in microtubule stabilization effects nearly identical to those of the taxoids.[5] The taccalonolides are unique in that they do not bind directly to microtubules/tubulin and do not enhance the polymerization of purified tubulin in biochemical assays.[6] The ability of the taccalonolides to cause microtubule stabilizing effects through a unique binding site and an entirely distinct mechanism of action prompted our interest in understanding this class of molecules.

Intense efforts over the past 3 decades have identified a large variety of interesting chemical compounds from the roots and rhizomes of *Tacca* species, including 25 taccalonolides, denoted as taccalonolides A−Y.[7−15] However, there have been limited biological studies on the taccalonolides. In 2003, we first reported the microtubule stabilizing activities of taccalonolides A and E.[16] Follow-up studies showed preliminary structure−activity relationships (SAR) for the antiproliferative activities of taccalonolides A, E, B, and N. The antiproliferative potencies of these four taccalonolides in HeLa cells were all in the mid-nanomolar range (190−644 nM).[17]

In this study we isolated three previously undescribed taccalonolides designated: Z (**5**), AA (**6**), and AB (**7**). The biological activities of these molecules, as well as of two previously isolated but biologically uncharacterized taccalonolides, R (**9**) and T (**8**), are presented. The mechanisms of action of all the taccalonolides were evaluated and compared to taccalonolides A and E. Each of these taccalonolides stabilizes cellular microtubules and causes mitotic accumulation of cancer cells with multiple abnormal mitotic spindles. The relative potencies of these

Received: June 13, 2011
Published: July 29, 2011

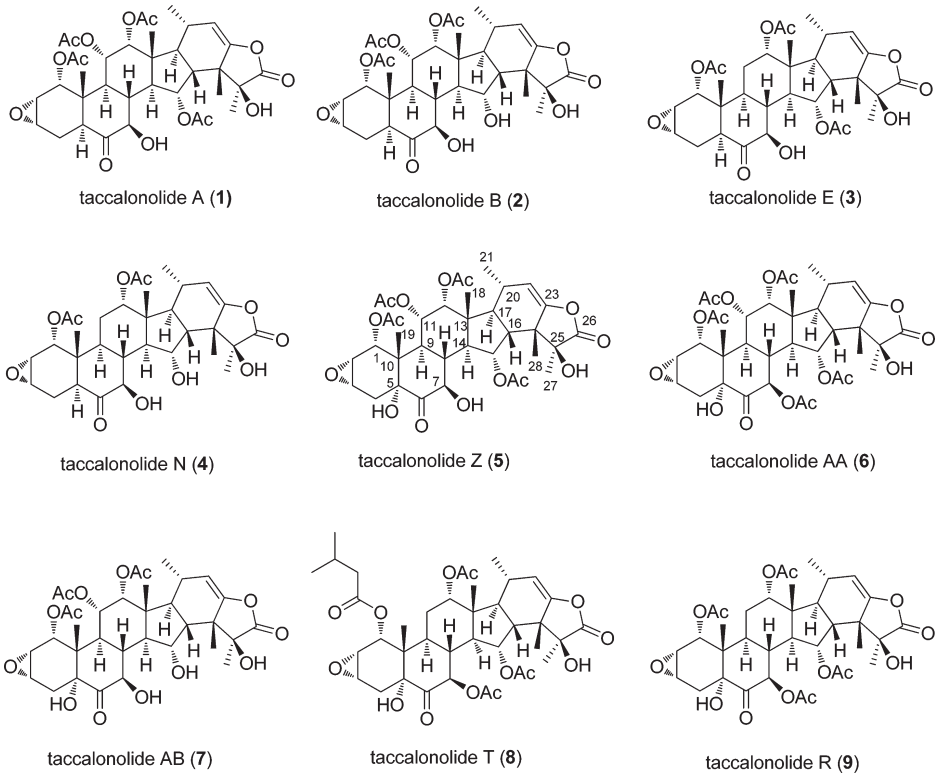

Figure 1. Structures of the taccalonolides.

taccalonolides range from 32 nM to 13 μM, offering a broad range of activity that provides an opportunity to explore SAR.

RESULTS AND DISCUSSION

Taccalonolide Isolation and Structure Elucidation. The roots and rhizomes of *T. chantrieri* and *T. integrifolia* were extracted using supercritical fluid CO_2 with methanol. After separation by flash chromatography using silica gel columns, normal and reverse phase HPLC was employed to obtain purified taccalonolides. Taccalonolides A (**1**), E (**3**), R (**9**), T (**8**), and AA (**6**) were isolated from *T. chantrieri*, while taccalonolide Z (**5**) was obtained from *T. integrifolia* (Figure 1). Mild base hydrolysis of taccalonolides A, E, and Z yielded taccalonolides B (**2**), N (**4**), and AB (**7**), respectively.

Taccalonolide Z (**5**) was obtained as a white powder. The proton NMR spectrum showed four acetyl signals at δ 2.16, 2.13, 2.00, 1.97, five methyl signals at δ 1.64 (s), 1.34 (s), 0.98 (s), 0.89 (d, J = 7.2 Hz), 0.73 (s), five oxygenated methine signals at δ 5.53 (t, J = 10.2 Hz), 5.23 (br), 5.22 (dd, J = 9.6, 2.4 Hz), 4.85 (d, J = 5.4 Hz), 4.73 (dd, J = 10.2, 5.4 Hz), two epoxyl methine signals at δ 3.74 (t, J = 4.5 Hz) and 3.61 (dt, J = 4.2, 1.8 Hz), one olefinic signal at δ 5.06 (d, J = 1.2 Hz). All these proton NMR data are similar to those of taccalonolide A and indicated that **5** is a taccalonolide type steroid. The molecular formula of $C_{36}H_{46}O_{15}$ was determined by HRMS of 719.2934 (calcd 719.2915), suggesting that **5** has one more oxygen than taccalonolide A (**1**). In addition, three signals for hydroxyl groups were observed at δ 3.64 (s), 3.45 (d, J = 5.4 Hz), and 2.58 (s), which is one more than taccalonolide A. The carbon-13 NMR showed seven oxygenated carbon signals at δ 79.08, 78.74, 74.13, 74.06, 71.20, 71.17, 71.14 and confirmed one more hydroxyl group for **5** compared to taccalonolide A. The ^3J HMBC correlation between the hydroxyl proton signal at δ 3.64 and the carbonyl carbon at δ 208.34 (C-6) suggested that the hydroxyl group is located at C-5. The configuration of this hydroxyl group was determined as α by the NOE correlations between 5-OH/H-7,9,4α. The other ^{1}H and ^{13}C NMR data for **5** are similar to those for **1**; thus, **5** was determined as 5α-hydroxytaccalonolide A, and this was confirmed by 2D NMR data. A trivial name taccalonolide Z was given to **5**, and its structure is shown in Figure 1.

Taccalonolide AA (**6**) was isolated as a white powder. The proton NMR spectrum of **6** showed characteristics almost identical to those of **5**, indicating a similar taccalonolide structure: five acetyl signals at δ 2.20, 2.15, 2.14, 2.00, 1.98, five methyl signals at δ 1.64 (s), 1.34 (s), 1.04 (s), 0.91 (d, J = 7.0 Hz), 0.72 (s), five acetoxylated methine signals at δ 5.72 (d, J = 11.0 Hz), 5.55 (d, J = 9.5 Hz), 5.25 (br), 5.23 (brd, J = 11.0 Hz), 4.91 (d, J = 5.0 Hz), two epoxyl methine signals at δ 3.72 (t, J = 4.5 Hz) and 3.59 (br), one olefinic signal at δ 5.09 (br). Taccalonolide AA (**6**) has one more acetyl signal than taccalonolide Z (**5**). The chemical shift of H-7 at δ 5.72 (d, J = 11.0 Hz) was ~0.99 ppm downfield than that of **5**, suggesting that this additional acetyl group was located at 7-OH. An HMBC correlation between H-7 and a carbonyl carbon at δ 170.8 confirmed this assignment. The other ^{1}H, ^{13}C, and 2D NMR data are similar to those for **5**; thus, the structure of **6** was determined as shown in Figure 1 and a trivial name taccalonolide AA was assigned.

Taccalonolide AB (**7**) was obtained as white powder. The LC/MS showed pseudomolecular ions at 677 $[M + H]^+$, 694 $[M + NH_4]^+$, and 699 $[M + Na]^+$, indicating the loss of an acetyl group from taccalonolide Z (**5**). The proton NMR showed the chemical shift of H-15 of **7** at δ 4.75 (ddd, J = 3.5, 9.0, 11.6 Hz), which is shifted 0.78 ppm upfield compared with that of **5**, suggesting the loss of acetyl group at 15-OH. The HMBC

dx.doi.org/10.1021/jm200757g |*J. Med. Chem.* 2011, 54, 6117–6124

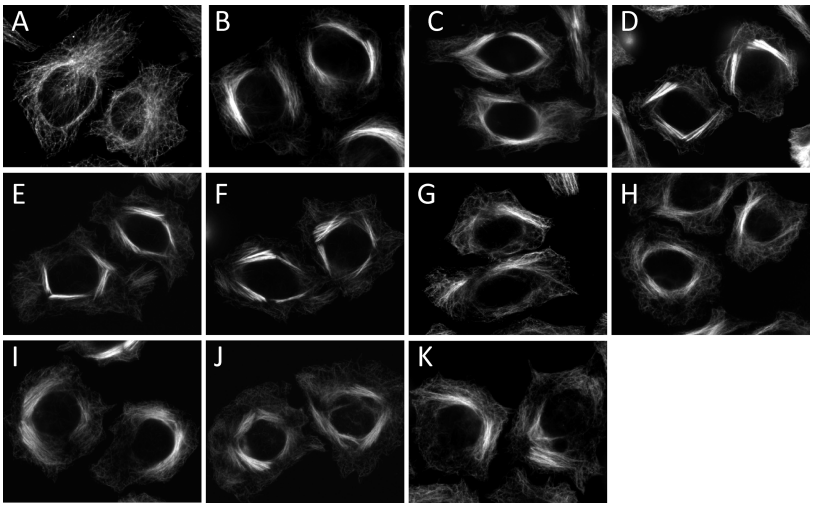

Figure 2. Effects of the taccalonolides on interphase cells. HeLa cells were treated for 18 h with vehicle (A), 0.5 μM paclitaxel (B), 3.5 μM taccalonolide A (C), 0.8 μM taccalonolide B (D), 2.5 μM taccalonolide E (E), 1.3 μM taccalonolide N (F), 57 μM taccalonolide R (G), 3.5 μM taccalonolide T (H), 0.6 μM taccalonolide Z (I), 0.32 μM taccalonolide AA (J), or 13.5 μM taccalonolide AB (K). Interphase microtubule structures were visualized by indirect immunofluorescence using a β-tubulin antibody.

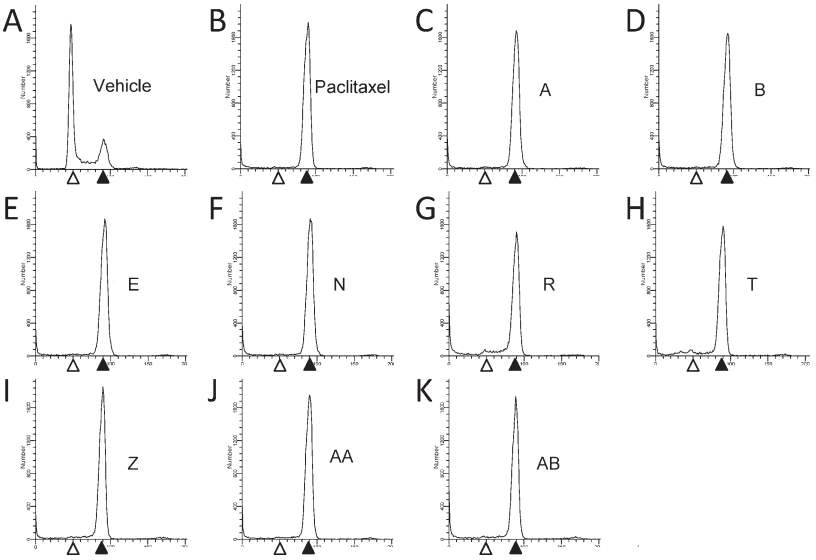

Figure 3. Effects of the taccalonolides on cell cycle distribution. HeLa cells were treated with vehicle (A), 12 nM paclitaxel (B), 3.5 μM taccalonolide A (C), 0.8 μM taccalonolide B (D), 2.5 μM taccalonolide E (E), 1.3 μM taccalonolide N (F), 111 μM taccalonolide R (G), 3.5 μM taccalonolide T (H), 0.6 μM taccalonolide Z (I), 0.32 μM taccalonolide AA (J), or 13.5 μM taccalonolide AB (K) for 18 h and stained with Kirshan's reagent. Open and filled arrowheads denote the populations of cells with 2N (G_1) and 4N (G_2/M) DNA content, respectively.

correlation between 15-OH (δ 4.94) and C-15 (δ 71.5) confirmed the assignment.

Microtubule Stabilization and Mitotic Arrest. The ability of the newly isolated taccalonolides to cause bundling of interphase microtubules was evaluated in HeLa cells. Consistent with the effects of taccalonolides A and E, which were shown to exert interphase microtubule bundling in previous studies,[16] taccalonolides B, N, R, T, Z, AA, and AB each caused the formation of thick bundled microtubule tufts typical of microtubule stabilizers including paclitaxel (Figure 2). Although microtubule stabilizers cause an increase in the density of interphase microtubules, the mechanism by which these agents inhibit the proliferation of cancer cells in vitro is widely accepted to be due to their ability to interrupt microtubule dynamics in mitosis, leading to mitotic arrest. The effect of the taccalonolides on mitotic progression was analyzed by flow cytometry. All nine taccalonolides caused an accumulation of cells in the G_2/M phase of the cell cycle with 4N DNA content (Figure 3). This accumulation is identical to the mitotic arrest that is observed after treatment of HeLa cells with paclitaxel (Figure 3).

The effects of the taccalonolides on mitotic spindle structures were evaluated to test whether they caused mitotic spindle defects leading to cell cycle arrest. β-Tubulin and DNA were visualized in HeLa cells by indirect immunofluorescence and DAPI staining, respectively. Most of the cells treated with each taccalonolide at the concentration that caused G_2/M accumulation were found to be in

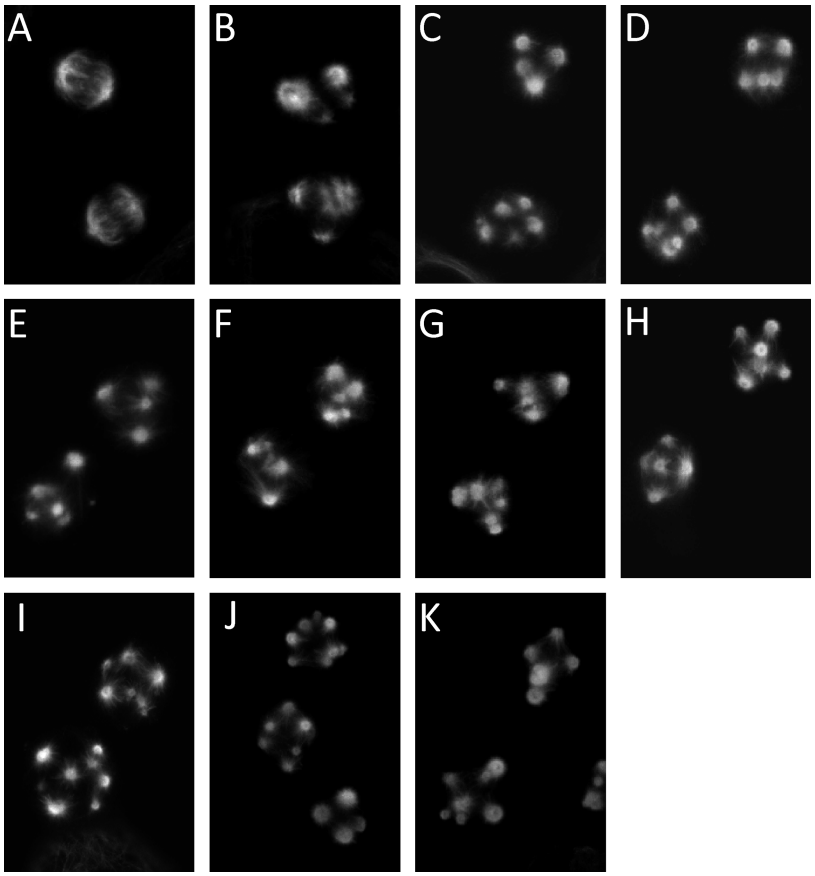

Figure 4. Effects of the taccalonolides on mitotic spindles. HeLa cells were treated for 18 h with vehicle (A), 12 nM paclitaxel (B), 3.5 μM taccalonolide A (C), 0.8 μM taccalonolide B (D), 2.5 μM taccalonolide E (E), 1.3 μM taccalonolide N (F), 57 μM taccalonolide R (G), 3.5 μM taccalonolide T (H), 0.6 μM taccalonolide Z (I), 0.32 μM taccalonolide AA (J), or 13.5 μM taccalonolide AB (K). The microtubule structures in mitotic cells were visualized by indirect immunofluorescence using a β-tubulin antibody.

Table 1. Antiproliferative Potency of Taccalonolides[a]

taccalonolide	IC_{50} (nM)
taccalonolide A	594 ± 43
taccalonolide B	190 ± 3
taccalonolide E	644 ± 10
taccalonolide N	247 ± 16
taccalonolide R	13144 ± 1390
taccalonolide T	335 ± 24
taccalonolide Z	120 ± 7.5
taccalonolide AA	32.3 ± 1.9
taccalonolide AB	2767 ± 107
paclitaxel	1.2 ± 0.1

[a] The concentration of each drug that causes 50% inhibition of cellular proliferation (IC_{50}) after 48 h of treatment was measured using the SRB assay (n = 3−5). IC_{50} values for taccalonolides A, E, B, and N are from Risinger et al.[17]

mitosis as evidenced by a "rounded up" cellular morphology and condensed DNA. These mitotic cells contained multiple abnormal mitotic spindles, which is another common effect of microtubule stabilizing agents (Figure 4). These findings demonstrate that all nine taccalonolides, A, B, E, N, R, T, Z, AA, and AB, are microtubule stabilizers that cause mitotic arrest of cells with multiple abnormal mitotic spindles.

Antiproliferative Activities of the Taccalonolides. The antiproliferative potencies of the taccalonolides were evaluated in HeLa cells using the SRB assay. The most potent taccalonolide is the newly identified taccalonolide AA, with an IC_{50} of 32.3 nM (Table 1). This makes taccalonolide AA the most potent taccalonolide identified thus far. This low nanomolar potency is closer to other naturally occurring microtubule stabilizers, including paclitaxel, the epothilones, laulimalide, and peloruside A, than the initially studied taccalonolides A and E.[17] Other taccalonolides that had IC_{50}s in the nanomolar range include taccalonolides Z (120 nM), B (190 nM), N (247 nM), T (335 nM), A (594 nM), and E (644 nM) (Table 1). Taccalonolides AB and R were significantly less potent, with IC_{50} values of 2.8 and 13.1 μM, respectively (Table 1). The 400-fold difference in activity between the most and least potent taccalonolides isolated provides the opportunity to explore the structure−activity relationships among the taccalonolides.

Structure−Activity of the Taccalonolides. Our previous work comparing the potency of taccalonolides A, B, E, and N in various drug sensitive and drug resistant cell lines gave a preliminary indication of the SAR of the taccalonolides, specifically the consequence of the presence or absence of an acetate group at C_{11} and/or C_{15}.[17] Taccalonolides A and E differ only by the respective presence or absence of an acetoxy group at the C_{11} position and they did not show major differences in potency, suggesting that this acetoxy functionality did not influence potency or microtubule stabilizing activity. Similarly,

Table 2. Antitumor Effects of Taccalonolides A, E, and N in the Mammary 16/C Model[a]

treatment	total dose (mg/kg)	T/C (%)	$T - C$ (day)	gross log cell kill	median (range) of tumor size (mg) and number of tumor-free mice on day 12	mean body weight loss (%)
no treatment	-	-	-	-	1029 (63−2827)	−2.2
paclitaxel	73.5	0	19	4.8	0 (all zero)	−6.3
taccalonolide A	56	0	16	4.0	0 (all zero)	−16.7[b]
taccalonolide A	40	24	4	1.0	256 (108−756)	−6.3
taccalonolide E	90	17	5	1.25	172 (0−947)	−4.1
					1/5 = 0	
taccalonolide E	54	81	1	0.25	837 (0−1755)	−2.0
					1/5 = 0	
taccalonolide N	36	0	5	1.25	(0−126)	−8.2
					3/5 = 0	
taccalonolide N	20	43	1	0.25	445 (0−2277)	−2.1
					1/5 = 0	

[a] T/C is the median tumor mass of a given treated group (T) divided by the median tumor mass of the control (C) and expressed as a percent. The tumor growth delay ($T - C$) is the median number of days between the time the treatment (T) and control (C) group tumors reach the predetermined size of 1000 mg. The gross log cell kill is calculated by $[(T - C)/3.32] \times$ Td, where Td is the tumor volume doubling time (in days). [b] A 20% lethality (1/5 mice) was observed at this dose.

taccalonolides B and N also differ from one another only by the presence or absence of an acetoxy group at C_{11} and showed comparable activity to one another. As evidenced by these two pairs of compounds, the presence or absence of the C_{11} acetoxy group did not have a large effect on potency.[17] Another SAR evaluation made possible with these two pairs of compounds is the contribution of the C_{15} acetate. Taccalonolides B and N are produced by mild base hydrolysis of the C_{15} acetate of taccalonolides A and E, respectively, resulting in a hydroxyl group at this position. A consistent increase in potency was observed upon hydrolysis of the C_{15} acetate as indicated by the 3.1-fold greater potency of taccalonolide B compared to A and the 2. 6-fold greater potency of taccalonolide N compared to E in HeLa cells.[17]

We now expanded the number of taccalonolides available for SAR analysis from four to nine by adding three new taccalonolides as well as two others that have not yet been evaluated for antiproliferative activities. Analysis of the potencies of these taccalonolides provided another opportunity to examine the effect of the C_{11} acetoxy group, since the only difference between taccalonolides AA and R is the presence of this acetoxy substituent in taccalonolide AA. In contrast to the relative unimportance of the C_{11} acetoxy moiety on potency between the taccalonolides A and E or B and N, this modification caused a 400-fold difference in potency between taccalonolides AA and R (Table 1). The other structural differences between this new pair of taccalonolides and taccalonolides A, E, B, N occur in the southern part of the molecule where there is a hydroxyl group at C_5 and an acetate at 7-OH (Figure 1). Therefore, it appears that these structural features in the southern portion of taccalonolides AA and R confer sensitivities to the constituents present at C_{11}. These data suggest that interactions across the molecule can influence the potency of a taccalonolide.

Another indication that the individual chemical substituents on the taccalonolide backbone interact in a complex manner to influence activity is shown by the effects of hydrolysis of the C_{15} acetate. As mentioned above, when this acetate is hydrolyzed in taccalonolide A or E, the resulting products, taccalonolides B and N, show a 2.6- to 3.1-fold increase in potency (Table 1).[17] However, when this same acetate is hydrolyzed in taccalonolide Z to yield taccalonolide AB, the potency is decreased by 23-fold (Table 1). Again, context is important because the only difference between taccalonolides Z and A is a hydroxyl group at the C_5 position (Figure 1). Finally, taccalonolide T is unique from the other taccalonolides evaluated in this study in that it contains a bulky isovalerate substituent at the C_1 position (Figure 1). This is the only difference between taccalonolides R and T and provides a dramatic 38-fold increase in potency (Table 1). It will be interesting to see whether adding steric bulk at this position has a consistent effect on potency in further studies.

These findings strongly suggest that the SAR for the taccalonolides is not simple and instead suggest that there are complex relationships among multiple sites on the taccalonolide backbone. On the basis of the limited data with these taccalonolides, we can categorize the taccalonolides into two groups, those with the 5-hydroxy group and those without the 5-hydroxy group. For taccalonolides without the 5-hydroxyl group, which include the taccalonolides A, B, E, and N, hydrolysis of the C_{15} acetate resulted in 2- to 3-fold increase in potency, and the C_{11} acetoxy group did not affect the activity. For taccalonolides with the 5-hydroxyl group, taccalonolides Z, AA, AB, T, and R, the presence of the C_{11} acetoxy group dramatically increased the activity (taccalonolide AA vs R), while hydrolysis of the C_{15} acetate decreased the activity (taccalonolide Z vs AB). Finally, adding bulk to the acetate at C_1 also increased potency (taccalonolide T vs R). Although there does not appear to be a clear link between potency and any particular chemical substituent on the taccalonolide backbone, these data highlight the importance of isolating additional taccalonolides and making directed chemical modifications to further probe the complex interactions across the molecule. In future studies we will probe the effects of introducing different bulky groups on C_1 together with acetoxy groups at C_{11} to find the best combination of substituents at these sites. For example, the addition of a bulky substituent at the C_1 of taccalonolide AA may further improve the potency. Other studies planned will further evaluate the roles of the different acetylating groups at C_7 and C_{15}.

In Vivo Antitumor Activity. Antitumor studies were conducted to evaluate the in vivo activity of taccalonolides A, E, and N. This evaluation is important since in vitro activity is not necessarily retained in vivo because of pharmacokinetic properties and drug metabolism. The syngeneic murine mammary carcinoma 16/C model was used because it is an incurable, rapidly growing tumor that provides a rigorous test of new agents.[18,19] A total dose of 73.5 mg/kg paclitaxel was used as a positive control, and as expected, it provided excellent antitumor effects with a 0% T/C, 19 day tumor growth delay ($T - C$), and 4.8 gross log cell kill (Table 2). In comparison, a total dose of 56 mg/kg taccalonolide A provided excellent antitumor activity with a 0% T/C, 16 day tumor growth delay ($T - C$), and 4.0 gross log cell kill (Table 2). However, with this dose and schedule, taccalonolide A also produced a 16.7% mean body weight loss and delayed toxicity with one lethality occurring 16 days after the final dose was administered. A lower dose of taccalonolide A (40 mg/kg total) was better tolerated but less effective, yielding a 24% T/C and 1.0 gross log cell kill (Table 2).

Taccalonolide E at a total dose of 90 mg/kg provided a 17% T/C and 1.25 gross log cell kill with a well-tolerated maximal 4.1% body weight loss. At a lower total dose of 54 mg/kg, taccalonolide E yielded an 81% T/C. Similarly, taccalonolide N at a total dose of 36 mg/kg generated a T/C of 0% and a 1.25 gross log cell kill, while the 20 mg/kg total dose was less effective with a T/C of 43% and a 0.25 gross log kill (Table 2). These data indicate that 56 mg/kg taccalonolide A provided the longest tumor growth delay ($T - C$) and the highest gross log cell kill of the taccalonolides tested in this trial. However, at this dose taccalonolide A was above the maximum tolerated dose (MTD) because it caused substantial weight loss and 20% lethality. Antitumor effects at doses over the MTD are difficult to interpret because they cannot be clearly separated from the toxic effects on the whole animal. However, a slightly lower total dose of taccalonolide A, 40 mg/kg, showed antitumor activity with low toxicity (Table 2). Additionally, in a previous study a 38 mg/kg total dose of taccalonolide A was highly effective against a drug resistant tumor and caused no drug deaths,[17] suggesting that taccalonolide A has a narrow therapeutic window. At the highest nontoxic doses tested, all the taccalonolides showed comparable antitumor activity, suggesting that the core structure of this class of molecules possesses antitumor activity that may be amenable to refinement and improvement through the isolation of additional taccalonolides and/or analogue development. Pharmacokinetic and metabolism studies are planned for the future to further understand the factors that affect in vivo efficacy of the taccalonolides.

EXPERIMENTAL SECTION

Chemistry. NMR spectra were recorded on a Bruker Avance 500, 600, or 700 MHz instrument equipped with CryoProbe and a Varian VNMRS 600 MHz instrument. All spectra were measured and reported in ppm using the residual solvent ($CDCl_3$) as an internal standard. The HR mass spectra were obtained using a Thermo Scientific LTQ Orbitrap mass spectrometer. IR data were obtained on a Bruker Vector 22 with a Specac Golden Gate ATR sampler. The UV spectra were measured on a Varian Cary 5000 UV−vis NIR spectrophotometer. TLC was performed on aluminum sheets (silica gel 60 F_{254}, Merck KGaA, Germany). HPLC was performed on a Waters Breeze HPLC system. LC/MS was conducted on a Waters Alliance 2695 HPLC module, 996 photodiode array detector, and Micromass Quattro triple quadrupole mass spectrometer equipped with ESI. The purities of all compounds were determined to be greater than 95% by LC/MS and NMR.

Plant Material. *Tacca chantreiri* and *T. integrifolia* plants were purchased from a commercial grower. The roots and rhizomes were collected from living plants and stored at −80 °C until lyophilized.

Extraction and Isolation of the Taccalonolides. Dried and pulverized rhizomes (2.3 kg) of *T. chantrieri* were extracted in several batches using supercritical CO_2 with MeOH. The crude extracts were washed with hexanes and extracted with CH_2Cl_2. The CH_2Cl_2 extracts were subjected to silica gel flash chromatography and eluted with hexances/isopropanol (82:18) to obtain the taccalonolide enriched fraction. This fraction (1.4 g) was further purified on a silica gel HPLC column and eluted with isooctane/isopropanol (81:19) to yield fractions 1−8. Taccalonolides A (**1**) and E (**3**) were obtained from fractions 2 and 4, respectively. Fraction 1 (33 mg) was separated on a C-18 HPLC column, eluting with a gradient of acetonitrile/H_2O from 30% to 80% over 40 min to yield 1.2 mg of taccalonolide AA (**6**) and 0.8 mg of taccalonolide T (**8**). Fraction 3 was purified on a silica gel flash column and eluted with CH_2Cl_2/acetone 85:15 to yield taccalonolide R (**9**).

The roots and rhizomes of *T. integrifolia* (1445 g) were extracted to yield 11.7 g of CH_2Cl_2 extract using the same method as *T. chantrieri*. The CH_2Cl_2 extract was purified by silica gel flash chromatography followed by repeated normal phase HPLC to yield 13.1 mg of taccalonolide Z (**5**).

Hydrolysis of the Taccalonolides. Taccalonolide A (40 mg) was dissolved in 4 mL of methanol, and to this solution 8 mL of 0.05 M sodium bicarbonate was added. The solution was stirred at room temperature for 44 h. The reaction solution was extracted with EtOAc and purified on HPLC to yield 25.8 mg of taccalonolide B (**2**). Taccalonolides N (**4**) and AB (**7**) were produced by hydrolysis of taccalonolides E (**3**) and Z (**5**), respectively, using the same method.

*Taccalonolide Z (**5**).* White powder. HRESIMS: m/z 719.2934 (calcd for $C_{36}H_{47}O_{15}$ 719.2915). ESIMS: m/z 719.4 $[M + H]^+$, 736.4 $[M + NH_4]^+$, 731.5 $[M + Na]^+$. ^1H NMR: δ (ppm) 5.53 (t, J = 9.8 Hz, H-15), 5.23 (br, H-12), 5.22 (dd, J = 9.6, 2.4 Hz, H-11), 5.06 (d, J = 1.5 Hz, H-22), 4.85 (d, J = 5.4 Hz, H-1), 4.73 (dd, J = 10.2, 5.1 Hz, H-7), 3.74 (t, J = 4.5 Hz, H-2), 3.64 (s, 5-OH), 3.61 (m, H-3), 3.45 (d, J = 5.2 Hz, 7-OH), 3.17 (t, J = 11.6 Hz, H-9), 2.58 (s, 25-OH), 2.57 (dd, J = 15.0, 1.6 Hz, H-4a), 2.52 (t, J = 10.1 Hz, H-14), 2.42 (dd, J = 13.4, 10.2 Hz, H-16), 2.23 (d, J = 16.7 Hz, H-4b), 2.16 (s, 3H, 1-OAc), 2.15 (m, H-20), 2.13 (s, 3H, 12-OAc), 2.00 (s, 3H, 15-OAc), 1.97 (s, 3H, 11-OAc), 1.81 (dd, J = 13.4, 9.8 Hz, H-17), 1.64 (s, 3H, H-27), 1.56 (q, J = 10.8 Hz, H-8), 1.34 (s, 3H, H-28), 0.98 (s, 3H, H-18), 0.89 (d, 3H, J = 7.2 Hz, H-21), 0.73 (s, 3H, H-19). ^{13}C NMR: δ (ppm) 208.34 (C-6), 178.10 (C-26), 172.07 (15-OAc), 170.85 (11-OAc), 169.40(1-OAc), 169.25 (12-OAc), 154.50 (C-23), 111.07 (C-22), 79.08 (C-5), 78.74 (C-25), 74.13 (C-12), 74.06 (C-1), 71.20 (C-15), 71.17 (C-7), 71.14 (C-11), 54.16 (C-14), 54.06 (C-3), 50.97 (C-16), 50.60 (C-2), 50.07 (C-24), 48.85 (C-17), 45.86 (C-10), 44.19 (C-8), 43.15 (C-13), 37.13 (C-9), 30.61 (C-20), 26.94 (C-4), 25.32 (C-28), 22.36 (15-OAc), 21.16 (11-OAc), 21.02 (12-OAc), 20.72 (1-OAc), 20.61 (C-27), 20.08 (C-21), 14.61 (C-19), 13.37 (C-18).

*Taccalonolide AA (**6**).* White powder. HRESIMS: m/z 761.3032 (calcd for $C_{38}H_{49}O_{16}$ 761.3021). ESIMS: m/z 761.4 $[M + H]^+$, 778.4 $[M + NH_4]^+$, 783.5 $[M + Na]^+$, 701.3 $[M - OAc]^+$. ^1H NMR: δ (ppm) 5.73 (d, J = 11.0 Hz, H-7), 5.55 (t, J = 9.4 Hz, H-15), 5.25 (d, J = 2.6 Hz, H-12), 5.23(dd, J = 11.7, 2.6 Hz, H-11), 5.09 (d, J = 1.4 Hz, H-21), 4.91 (d, J = 5.5 Hz, H-1), 3.72 (t, J = 4.5 Hz, H-2), 3.61 (s, 5-OH), 3.59 (m, H-3), 3.30 (t, J = 11.4 Hz, H-9), 2.63 (t, J = 10.0 Hz, H-14), 2.62 (s, 25-OH), 2.56 (brd, J = 14.5 Hz, H-4a), 2.43 (dd, J = 13.4, 9.8 Hz, H-16), 2.20 (s, 3H, 1-OAc), 2.19 (m, H-4b), 2.17 (m, H-20), 2.16 (s, 3H, 11-OAc), 2.15 (s, 3H, 12-OAc), 2.03 (q, J = 11.0 Hz, H-8), 2.00 (s, 3H, 7-OAc), 1.98 (s, 3H, 15-OAc), 1.65 (s, 3H, H-27), 1.33 (s, 3H, H-28), 1.04 (s, 3H, H-18), 0.92 (s, 3H, H-21), 0.73(s, 3H, H-18). ^{13}C NMR:

δ (ppm) 201.65 (C-6), 178.04 (C-25), 172.10 (15-OAc), 170.88 (11-OAc), 170.76 (7-OAc), 169.51 (1-OAc), 169.33 (12-OAc), 154.34 (C-23), 111.33 (C-22), 79.76 (C-5), 79.10 (C-26), 74.31 (C-7), 74.26 (C-1), 73.99 (C-12), 71.54 (11), 71.22 (C-15), 54.34 (14), 54.22 (C-3), 51.60 (C-16), 50.60 (C-2), 50.26 (C-24), 48.66 (C-17), 45.64 (C-10), 43.61 (C-13), 39.48 (C-8), 38.57 (C-9), 30.75 (C-20), 26.78 (C-4), 25.37 (C-28), 22.79 (15-OAc), 21.27 (7-OAc), 21.23 (12-OAc), 21.19 (11-OAc), 20.97 (1-OAc), 20.68 (C-21), 20.21 (C-27), 14.88 (C-19), 13.74 (C-18).

Taccalonolide AB (7). White powder. HRESIMS: *m/z* 677.2814 (calcd for $C_{34}H_{45}O_{14}$ 677.2809). ESIMS: 677.4 $[M + H]^+$, 694.4 $[M + NH_4]^+$, and 699.4 $[M + Na]^+$. ^{1}H NMR: δ (ppm) 5.27 (dd, *J* = 11.9, 2.1 Hz, H-11), 5.22 (d, *J* = 2.1 Hz, H-12), 5.01 (br, H-21), 4.93 (d, *J* = 3.6 Hz, 15-OH), 4.91 (dd, *J* = 10.8, 4.6 Hz, H-7), 4.83 (d, *J* = 5.4 Hz, H-1), 4.62 (br, 25-OH), 4.47 (ddd, *J* = 11.1, 9.0, 3.4 Hz, H-15), 4.05 (d, *J* = 4.5 Hz, 7-OH), 3.76 (t, *J* = 4.5 Hz, H-2), 3.69 (s, 5-OH), 3.63 (m, H-3), 3.17 (t, *J* = 11.6 Hz, H-9), 2.56 (brd, *J* = 15.7 Hz, H-4a), 2.43 (dd, *J* = 13.0, 11.0 Hz, H-16), 2.26 (m, *J* = 16.8 Hz, H-4b), 2.24 (m, H-14),2.17 (s, 3H, 1-OAc), 2.15 (m, H-20), 2.14 (s, 3H, 12-OAc), 1.99 (s, 3H, 11-OAc), 1.86 (dd, *J* = 13.2, 9.9 Hz, H-17), 1.69 (s, 3H, H-27), 1.64 (q, *J* = 10.9 Hz, H-8), 1.37 (s, 3H, H-28), 0.97 (s, 3H, H-18), 0.89 (d, 3H, *J* = 7.0 Hz, H-21), 0.78 (s, 3H, H-19). ^{13}C NMR: δ (ppm) 207.23 (C-6), 175.35 (C-26), 171.12 (12-OAc), 169.64 9 (1-OAc), 169.51 (12-OAc), 154.90 (C-22), 110.43 (C-21), 79.10 (C-25), 78.75 (C-5), 74.41 (C-12), 74.12 (C-1), 72.04 (C-7), 71.46 (C-15), 70.89 (C-11), 57.57 (C-14), 54.12 (C-3), 51.04 (C-24), 50.79 (C-2), 50.28 (C-16), 48.19 (C-17), 46.06 (C-10), 44.06 (C-14), 43.82 (C-8), 36.66 (C-9), 31.17 (C-20), 27.07 (C-4), 25.62 (C-28), 21.99 (C-27), 21.35 (12-OAc), 21.14 (11-OAc), 20.83 (1-OAc), 20.30 (C-21), 14.70 (C-19), 13.44 (C-18).

Cell Culture. The HeLa cervical cancer cell line was obtained from American Type Tissue Culture Collection (Manassas, VA) and grown in Basal Media Eagle (BME) medium (Invitrogen; Carlsbad, CA) supplemented with 10% fetal bovine serum (Hyclone; Logan, UT) and 50 μg/mL gentamicin sulfate (Invitrogen).

Inhibition of Cellular Proliferation. The antiproliferative effects of the taccalonolides were evaluated using the SRB assay[20] as previously described.[16] The concentration of drug that caused a 50% inhibition of cellular proliferation (IC_{50}) was calculated from the linear portion of the log of the dose response curve. Each IC_{50} represents the mean and standard deviation of three to five independent experiments, each performed in triplicate. Paclitaxel is included as a reference compound. The determination of IC_{50} values was performed on taccalonolide material after NMR analysis and subsequent lyophilization. Ethanol was used as the vehicle for all cellular studies.

Immunofluorescence. Cellular microtubules in interphase or mitotic HeLa cells were visualized using indirect immunofluorescence techniques as previously described.[16] Cells were treated for 18 h with vehicle, a taccalonolide, or the positive control paclitaxel, fixed with methanol and microtubules visualized with a β-tubulin antibody. Representative images of interphase and mitotic cells were acquired using a Nikon Eclipse 80i fluorescence microscope and compiled using NIS Elements AR 3.0 software. Concentrations of taccalonolides that caused similar levels of mitotic arrest at 18 h were used (5−10× their IC_{50} values). Paclitaxel requires a substantially higher concentration, 400× the IC_{50}, to initiate interphase bundling.

Flow Cytometry. HeLa cells were incubated for 18 h with vehicle, each taccalonolide or paclitaxel as a positive control. The cells were harvested, and the DNA was stained with propidium iodide using Krishan's reagent.[21] Cellular DNA content was analyzed using a FACS Calibur flow cytometer (BD Biosciences). Data were plotted as propidium iodide intensity versus the number of events using ModFit LT 3.0 software (Verity Software, Topsham, ME). Concentrations of paclitaxel or taccalonolide that caused similar levels of mitotic arrest at 18 h were used (5−10× their IC_{50} values).

In Vivo Testing. The antitumor efficacies of taccalonolides A, E, and N were evaluated in the murine syngeneic Mammary 16/C model.[18] The average mouse weight was 19.3 ± 1.0 g at the start of treatment. Tumor fragments were bilaterally implanted subcutaneously in female B_6C_3F1 (C57BL6 × C3H) mice on day 0, then nonselectively distributed to the various treatment and control groups (*n* = 5 mice/group). All drugs were administered by iv in a 0.2 mL volume. The taccalonolides were solubilized in 50% DMSO/50% Cremophor to generate stocks of 10.0−12.1 mg/mL and then diluted with sterile water for injections. Paclitaxel (Mayne Pharma; Salisbury South, SA, Australia) was diluted with water from clinical grade stocks to a final concentration of 6 mg/mL.

The protocol design and antitumor efficacy analyses were performed as described previously.[19] The scheduling was based on our prior studies to optimize antitumor activity and reduce toxicity. Each taccalonolide was administered intravenously on days 1, 4, and 6 with an additional dose 2−3 days later for taccalonolides A and N. Taccalonolide E treatments were also administered on days 8, 9, and 11 because the weight loss was least severe in this treatment group. Mice were weighed and observed daily, and tumor size was measured two to three times weekly. Tumor mass was calculated using the followng formula: mass (mg) = length (mm) × [width (mm)]^2/2. Antitumor efficacy was evaluated by the following standard calculations. (1) % *T*/*C*: The median tumor mass of a given treated group (*T*) divided by the median tumor mass of the control (*C*), expressed as percent. The % *T*/*C* determination includes "zeros" and is made when the control group tumors reach exponential growth at approximately 700−1200 mg in size. (2) Tumor growth delay (*T* − *C*) and tumor cell kill: These measurements are quantitative determinations of antitumor activity. (*T* − *C*) is the median number of days between the time the treatment (*T*) and control (*C*) group tumors reach the predetermined size of 1000 mg. Tumor free survivors are excluded from this calculation and are tabulated separately. Tumor cell kill is determined using tumor growth delay (*T* − *C*) as described above in the following formula: gross log cell kill = [(*T* − *C*)/3.32] × Td, where Td is the tumor volume doubling time (in days) estimated from the best fit straight line from a log-linear growth plot of control group tumors in the exponential growth phase.

The mice were purchased from the NCI—Frederick Animal Production Program (Frederick, MD), housed in an AALAC-approved facility under fully licensed veterinary care (Wayne State University, Detroit, MI), and provided water and food ad libitum.

■ ASSOCIATED CONTENT

Supporting Information. 1D and 2D NMR spectra of compounds **5**, **6**, and **7**. This material is available free of charge via the Internet at http://pubs.acs.org.

■ AUTHOR INFORMATION

Corresponding Author

*For S.L.M: Phone: (210) 567-4788. Fax: (210) 567-4300. E-mail: Mooberry@uthscsa.edu. For J.P.: Phone: (210) 567-6267. Fax: (210) 567-4300. E-mail: Pengj2@uthscsa.edu.

■ ACKNOWLEDGMENT

This work was supported by NCI Grant CA121138 (S.L.M.), DOD-CDMRP Postdoctoral Award BC087466 (A.L.R.), and NCI Grant P30 CA054174 (S.L.M.).

■ ABBREVIATIONS USED

HSQC, heteronuclear single quantum coherence; HMBC, heteronuclear multibond correlation spectroscopy; SAR, structure−activity relationship

REFERENCES

(1) Fojo, T.; Menefee, M. Mechanisms of multidrug resistance: the potential role of microtubule-stabilizing agents. *Ann. Oncol.* **2007**, *18* (Suppl. 5), v3–8.

(2) Morris, P. G.; Fornier, M. N. Microtubule active agents: beyond the taxane frontier. *Clin. Cancer Res.* **2008**, *14*, 7167–7172.

(3) Galsky, M. D.; Dritselis, A.; Kirkpatrick, P.; Oh, W. K. Cabazitaxel. *Nat. Rev. Drug Discovery* **2010**, *9*, 677–678.

(4) Nogales, E.; Wolf, S. G.; Khan, I. A.; Luduena, R. F.; Downing, K. H. Structure of tubulin at 6.5 Å and location of the Taxol-binding site. *Nature* **1995**, *375*, 424–427.

(5) Bennett, M. J.; Barakat, K.; Huzil, J. T.; Tuszynski, J.; Schriemer, D. C. Discovery and characterization of the laulimalide-microtubule binding mode by mass shift perturbation mapping. *Chem. Biol.* **2010**, *17*, 725–734.

(6) Buey, R. M.; Barasoain, I.; Jackson, E.; Meyer, A.; Giannakakou, P.; Paterson, I.; Mooberry, S.; Andreu, J. M.; Diaz, J. F. Microtubule interactions with chemically diverse stabilizing agents: thermodynamics of binding to the paclitaxel site predicts cytotoxicity. *Chem. Biol.* **2005**, *12*, 1269–1279.

(7) Chen, Z.; Wang, B.; Chen, M. Steroidal bitter principles from tacca plantaginea structures of taccalonolide A and B. *Tetrahedron Lett.* **1987**, *28*, 1673–1676.

(8) Chen, Z.; Wang, B.; Shen, J. Taccalonolide C and D, two pentacyclic steroids of *Tacca plantaginea*. *Phytochemistry* **1988**, *27*, 2999–3002.

(9) Shen, J.; Chen, Z.; Gao, Y. The pentacyclic steroidal constituents of *Tacca plantaginea*: taccalonolides E and F. *Chin. J. Chem.* **1991**, *9*, 92–94.

(10) Shen, J.; Chen, Z.; Gao, Y. Taccalonolides from *Tacca plantaginea*. *Phytochemistry* **1996**, *42*, 891–893.

(11) Chen, Z.; Shen, J.; Gao, Y.; Wichtl, M. Five taccalonolides from *Tacca plantaginea*. *Planta Med.* **1997**, *63*, 40–43.

(12) Muhlbauer, A.; Gehling, M.; Velten, R.; Andersch, W.; Erdelen, C.; Harder, A.; Marczok, P.; Nauen, R.; Turberg, A.; Tran, V. S.; Adam, G.; Liu, J. Isolation and Preparation of Taccalonolides for Controlling Animal Pests. PCT Int. Appl. WO2001040256 A1 20010607, 2001.

(13) Huang, Y.; Liu, J. Three novel taccalonolides from the tropical plant *Tacca subflaellata*. *Helv. Chim. Acta* **2002**, *85*, 2553–2558.

(14) Muhlbauer, A.; Seip, S. Five novel taccalonolides from the roots of the vietnamese plant *Tacca paxiana*. *Helv. Chim. Acta* **2003**, *86*, 2065–2072.

(15) Yang, J.; Zhao, R.; Chen, C.; Ni, W.; Teng, F.; Hao, X.; Liu, H. Taccalonolides W−Y, three new pentacyclic steroids from *Tacca plantaginea*. *Helv. Chim. Acta* **2008**, *91*, 1077–1082.

(16) Tinley, T. L.; Randall-Hlubek, D. A.; Leal, R. M.; Jackson, E. M.; Cessac, J. W.; Quada, J. C., Jr.; Hemscheidt, T. K.; Mooberry, S. L. Taccalonolides E and A: plant-derived steroids with microtubule-stabilizing activity. *Cancer Res.* **2003**, *63*, 3211–3220.

(17) Risinger, A. L.; Jackson, E. M.; Polin, L. A.; Helms, G. L.; LeBoeuf, D. A.; Joe, P. A.; Hopper-Borge, E.; Luduena, R. F.; Kruh, G. D.; Mooberry, S. L. The taccalonolides: microtubule stabilizers that circumvent clinically relevant taxane resistance mechanisms. *Cancer Res.* **2008**, *68*, 8881–8888.

(18) Corbett, T. H.; Griswold, D. P., Jr.; Roberts, B. J.; Peckham, J. C.; Schabel, F. M., Jr. Biology and therapeutic response of a mouse mammary adenocarcinoma (16/C) and its potential as a model for surgical adjuvant chemotherapy. *Cancer Treat. Rep.* **1978**, *62*, 1471–1488.

(19) Polin, L.; Corbett, T.; Roberts, B. J.; Lawson, A. J.; Leopold, W. R., III; White, K.; Kushner, J.; Paluch, J.; Hazeldine, S.; Moore, R.; Rake, J.; Horwitz, J. P. *Transplantable Syngeneic Rodent Tumors: Solid Tumors of Mice*, 2nd ed.; Humana Press Inc.: Totowa, NJ, 2011; pp 43−78.

(20) Skehan, P.; Storeng, R.; Scudiero, D.; Monks, A.; McMahon, J.; Vistica, D.; Warren, J. T.; Bokesch, H.; Kenney, S.; Boyd, M. R. New colorimetric cytotoxicity assay for anticancer-drug screening. *J. Natl. Cancer. Inst.* **1990**, *82*, 1107–1112.

(21) Krishan, A. Rapid flow cytofluorometric analysis of mammalian cell cycle by propidium iodide staining. *J. Cell Biol.* **1975**, *66*, 188–193.